

OZONE FORMATION DURING AN EPISODE OVER EUROPE :
A 3-D CHEMICAL/TRANSPORT MODEL SIMULATION

Terje Berntsen and Ivar S. A. Isaksen

Institute of Geophysics,
University of Oslo,
P.O.Box 1022, Blindern,
N-0315 Oslo, Norway

ABSTRACT

A 3D regional photochemical tracer/transport model for Europe and the Eastern North Atlantic has been developed based on the NASA/GISS CTM. The model resolution is 4x5 degrees latitude and longitude with 9 layers in the vertical (7 in the troposphere). Advective winds, convection statistics and other meteorological data from the NASA/GISS GCM are used. An extensive gas-phase chemical scheme based on the scheme used in our global 2D model has been incorporated in the 3D model. In this work ozone formation in the troposphere is studied with the 3D model during a 5 day periode starting June 30. Extensive local ozone production is found and the relationship between the source regions and the downwind areas are discussed. Variations in local ozone formation as a function of total emission rate, as well as the composition of the emissions (HC/NO_x ratio and isoprene emissions) are elucidated. An important vertical transport process in the troposphere is by convective clouds. The 3D model includes an explicit parameterization of this process. It is shown that this process has significant influence on the calculated surface ozone concentrations.

1 Introduction

Ozone formation in the troposphere over Europe and other industrialized regions leading to ambient concentrations well above health standards during periods with high pressure weather situations, is now a well established fact (Guicherit; 1988). The increase is observed at urban as well as rural locations. Measurements (Kley et al.; 88) show that typical ozone values have increased from 5-15 ppbv at turn of the century, to 30-40 ppbv at present most probably due to increased man made emissions of NO_x and hydrocarbons.

Several model studies have been performed to study this effect. This include box models, 1D and 2D eulerian models. Up to recently, lack of computer resources has put severe restrictions on the chemical scheme as well as the area and resolution of the models. The approach has been either to do regional studies with rather comprehensive chemical schemes (Chang et al.; 87), or global studies with simpler schemes (Crutzen and Zimmermann ; 91). This paper presents results from a 3D model with an extensive chemical scheme covering an area from 25°W to 55°E and 24°N to 76°N. The model is intended to be extended to a global scale after development and testing on less computer costly scales.

2 Model description

2.1 Transport

The model was originally developed by Prather et al.(87) to simulate global distribution and temporal variability of CFCs. As consistent global data sets with real-time meteorological data from numerical weather prediction models are not available, the model is set up to use data from the free running NASA/GISS general circulation model (GCM).

In this study calculations are done for a European "window" (25°W to 55°E and 24°N to 76°N) with a resolution of 5° longitude and 4° latitude. In the vertical there are 9 layers (σ -coordinates, $\sigma = (P - P_T)/(P_s - P_T)$) between the surface and 10 hPa. Table 1 gives the vertical resolution.

σ	1.0	.95	.87	.73	.55
P (hPa)	984	934	854	720	550
Z (km)	0.0	0.5	1.2	2.7	4.9
σ	0.39	0.25	0.14	0.061	0.0
P (hPa)	390	255	150	70	10
Z (km)	7.4	10.3	13.7	18.5	31.2

Table 1: Horizontal boundaries of the 9 layers in the model. $P_s = 984$ hPa is the mean surface pressure in the GCM.

The meteorological data consist of 4 hour integrated values of horizontal mass fluxes and surface pressure, total optical depth, surface precipitation and number of convective events (see Prather et al.;87). Temperature, humidity, precipitation (from cumulus convection and large scale precipitation) are given as 5 day averages from the GCM. Tracer transport due to convection is calculated by a mass flux scheme which divide the convection into three classes (dry, moist/shallow and moist/deep).

The advection of tracers are solved numerically by the method of conservation of second order moments (Prather; 86). A timestep of one hour is applied in calculation of the advective transport.

2.2 Chemistry

The model has been expanded to include an extended ozone chemistry scheme. It includes a gas-phase chemistry with first order scavenging of water soluble species. The scheme follows the basic pattern of the scheme developed for use in our global 2D model (Isaksen and Hov; 87), with recent updates of reaction mechanisms and rates according to IUPAC (89),

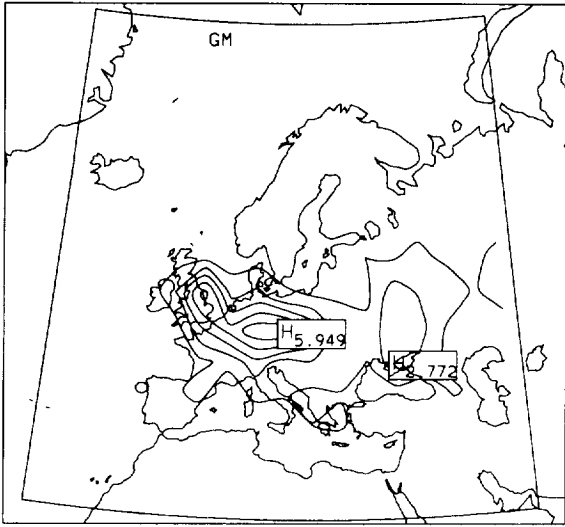


Figure 1: Relative distribution of NO emissions. Numbers give percentage pr. grid square of the total NO-emission which is 9.35 Tg/y as NO.

NASA/JPL (90) and Atkinson (90). The scheme includes 45 components, 16 photolytical reactions and 91 thermal reactions. The quasi steady state approximation (QSSA) of Hesstvedt et al. (78) is applied to solve the scheme, with a timestep of one hour.

Photolysis rates are calculated by the two-stream approximation method of Isaksen et al. (77) with corrections for diffusive scattering (Jonson and Isaksen ; 91) for a clear sky situation. Modifications of photolysis rates due to clouds are calculated according to the parameterization given by Chang et al.(87). To run a 5 day simulation on a DEC-station 5000/200 takes about 45 minutes CPU-time.

2.3 Emissions

Reasonable emission rates of primary pollutants are crucial if the model shall be able to simulate the real atmosphere. Table 2 gives the emission rates of the primary pollutants (except isoprene). Emission rates and geographical distribution of NO_x and hydrocarbons are derived on the basis of data from EMEP (D.Simpson,private com.) and EPA (Watson et al.;91). In the EMEP data hydrocarbon emissions are given as total man made VOC, while the EPA data divide the VOC emissions into groups such as paraffins, olefins, aromats, etc., but on a much courser grid (10° × 10°). The total VOC emissions were therefore taken from EMEP, while the spieciation was done according to the EPA data. However there was considerable differences between the total emission rates in the two sets of emission data, which means that this is a very significant source to uncertainties in the results. Fig. 1 and 2 show the relative distribution of NO and C₂H₆ emissions applied in the model. In this study no daily variation in the emissions are included (except for isoprene), nor any emissions from sources above the ground (airplanes and lightning).

Isoprene emissions are parameterized as a function of sunlight, surface temperature and deciduous forest cover according to Lubkert and Schopp (1989) and Veldt (1988):

$$E(\text{kg/h} * \text{km}^2) = 10^{(0.1 * T_s - 2.15)}$$

E is the hourly emission rate of isoprene in kg km⁻² h⁻¹ during

NO	NO ₂	CO	C ₂ H ₆	C ₄ H ₁₀
9.4	0.44	124.0	10.9	6.5
C ₆ H ₁₄	C ₂ H ₄	C ₃ H ₆	m-Xylene	HCHO
4.3	4.4	1.9	4.5	0.67

Table 2: Total emission rates applied in the model (except for isoprene). All values are in Tg/y of the emitted species.

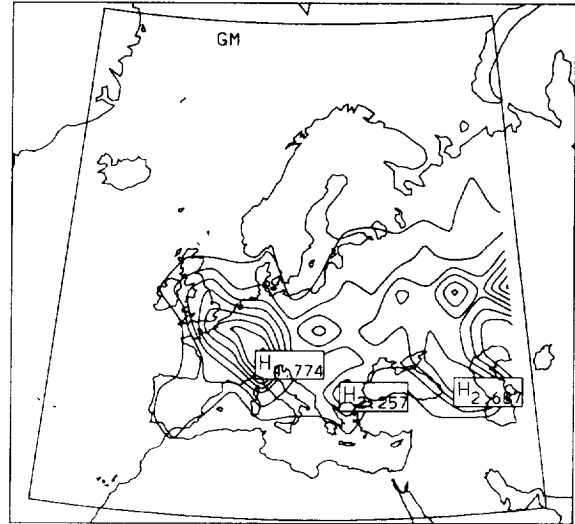


Figure 2: Relative distribution of C₂H₆ emissions. Numbers give percentage pr. grid square of the total C₂H₆-emission which is 10.9 Tg/y.

daytime, and T, is the ambient temperature in deg. C.

The data from the NASA/GISS GCM only include 5 day averaged temperatures, so a daily variation in the surface temperature (T_s) as a function of the local time (tt), with an amplitude of 10 deg. C has been included

$$T_s = 5.0 * \text{SIN}(\text{MOD}((tt + 24 - 10), 24) * 2\pi/24.0) + T(\text{GCM})$$

Fig. 3 shows the calculated relative distribution of isoprene emissions at 15 GMT. The very pronounced maximum results from a combination of very dense forest cover and high surface temperature during the 5 day period. As isoprene emissions are highly uncertain this maximum can at least serve as sensitivity test of the impact of biogenic emissions.

2.4 Boundary conditions and initialization

With such a limited model area, the results will be very sensitive to the fluxes across the vertical boundaries of the model.

The boundary concentration of the species are obtained from results from a 2D channel model (Solberg et al.; 89) covering a zonal band between 30°N and 60°N, and a 2D zonally averaged global model (Isaksen and Hov; 87). The results from the channel model are distributed latitudinally according to the relative latitudinal distribution in the 2D global model to obtain a 3D distribution which can be used to initiate the model, and as boundary conditions. To account for the possibility of a polluted air mass being transported out of the model area and back

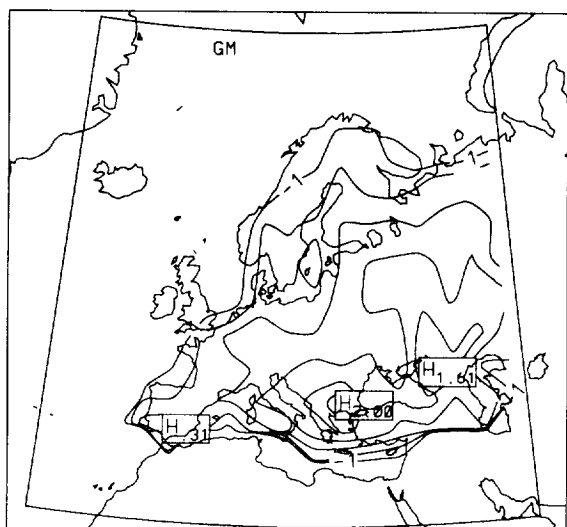
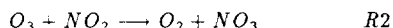
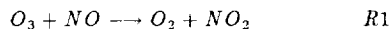


Figure 3: Relative distribution (%) at 15 GMT of the surface flux of isoprene. Numbers are on logarithmic scale relative to the grid cell with largest flux ($2.9 \cdot 10^{11}$ molec/($\text{cm}^2 \text{ s}$))

again due to a sudden shift in the wind direction, the boundary concentrations approach the upwind concentrations during out-flow and return to the original concentrations during a 12 hour relaxation period.

3 Results

The model has been run for a 5 day period starting at midnight GMT June 30. Fig. 4 shows the calculated surface concentration of ozone at 13 GMT the 5th day of the simulation. There is a broad maximum of about 70 ppbv over Northwestern Europe and the British Isles, and a secondary maximum over Eastern Europe. Earlier in the day the maximum is shifted towards the east with maximum values at about the same level (table 3) Fig. 5 shows the calculated ozone concentrations (mean of the two lowest layers in the model) at 4 different locations during the 5 day period. In the main source regions ozone concentrations show a very pronounced diurnal variation with a maximum concentration occurring usually before noon. The most important reason for the night time reduction is surface deposition ($\geq 50\%$ of the loss) and reactions with NO_x ($R1 \approx 20\%$ and $R2 \approx 25\%$ in the regions with large NO_x emissions).



The maximum surface concentration is very sensitive to the ventilation of the boundary layer through convective transport. As convective transport is only calculated every 4th hour, primary pollutants and their products (ozone, PAN etc.) are allowed to build up during the intervals between the convective events. This effect might give rise to regular over and under predictions, especially in the lowest layer of the model.

The surface ozone concentration and in particular the daily maximum is to a large degree determined by the composition of the emissions. To analyse the sensitivity of the model to variations in the emission rates and composition, several perturbations have been performed. Table 3 shows the maximum ozone concentration during the 5th day of the simulation at 4 locations. The locations were chosen to represent typical source regions.

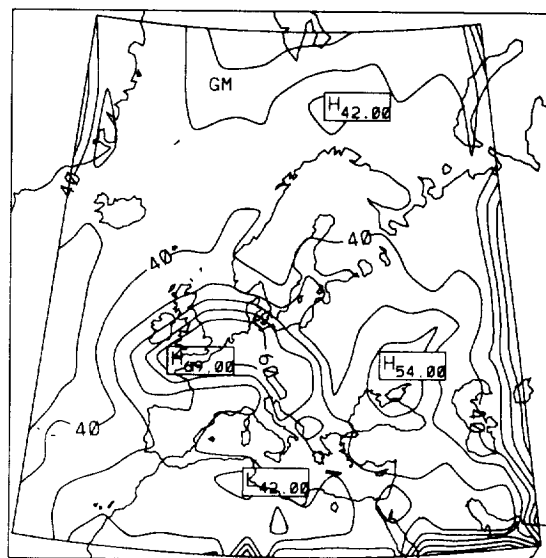


Figure 4: Calculated surface concentration (ppbv) of ozone at 13 GMT on 5th day of the simulation.

Over Western Europe, represented in fig.5 and table 3 by the grid cell located at 50°N and 5°E , NO_x emissions are large and the potential for further photochemical ozone production if NO_x emissions increase is low. In some cases it might even be negative, because reaction R1 followed by R3 consumes O_3 (and OH) faster than it is produced by R4-R6. The limiting factor for ozone production is then the abundance of RO_2 radicals (organic peroxy radicals and HO_2) which is produced by oxidation of hydrocarbons and CO by the OH radical.



In a region with a larger fraction of hydrocarbons in the emissions (42°N , 25°E) there is a large potential for further ozone production if NO_x emissions are increased. In this gridcell surface NO_x concentration stay around 0.5 ppbv during the periode from 10 am to 8 pm, while at the more polluted area over the Netherlands the corresponding NO_x concentration is around 2.5 ppbv. Table 3 shows that an increase of 50% in the NO_x emissions gives rise to an increase in the calculated surface ozone of 15%.

Over Eastern Europe (50°N , 25°E) the ratio HC/NO_x in the emissions are higher than in the west. It is therefore a potential for further ozone production if NO_x emissions are increased. A 13% increase in daily maximum ozone at the surface is calculated for a 50% increase in the NO_x emissions.

At the Scandinavian site (62°N , 15°E) there are small diurnal variations in the ozone concentration after the first day, and the concentration is virtually insensitive to the various perturbations of the emissions. Analysis show that there is net in situ loss of ozone all the time during this periode, and a steady-state situation between the local loss processes and transport is established within a few days. However this probably points to an underestimation of the emissions of precursors in this region as observations show evidence of significant ozone production at Scandinavian stations (Grennfeldt et al.,87).

Perturbation	O ₃ (ppb) at (°N, °E)			
	50,5	42,25	50,35	62,15
Reference	65	79	56	38
CH ₄ conc. = 0	61	78	55	38
Isoprene em. = 0	64	61	55	38
NMHC em. * 2	74	83	66	39
NO _x em. * 1.5	65	90	63	38
NO _x em. * 0.5	63	65	56	38

Table 3: Maximum calculated concentration of ozone (ppbv) in the lowest level during the 5 th day at 4 locations.

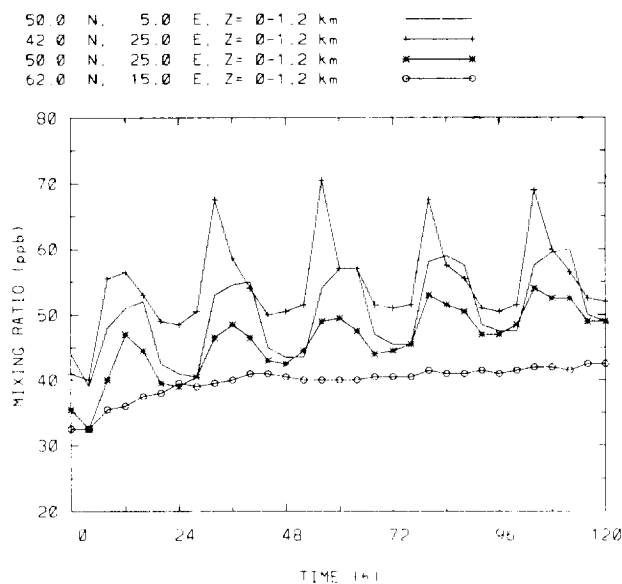


Figure 5: Calculated time development of ozone in the two lowest layers ($Z \approx 0-1.2$ km) at four locations during the 5 day simulation.

4 Conclusion

We have developed a 3D chemical tracer model based on the NASA/GISS CTM (Prather et al.; 87) for an extended European region with a comprehensive chemical scheme developed to study formation of photochemical oxidants. The model has been run for a 5 day period in the beginning of July, and the results are in general agreement with observations of ozone typical for this time of the year. Several perturbations have been performed, and the sensitivity of the model is consistent with other model studies. With some refinements of the model (especially with respect to convection) and improvement of the emission database, the model should be well suited to study the processes governing the formation of photochemical oxidants on regional scales.

Acknowledgement

This project was supported by BP-Norway Limited U.A. Contract No. C-550088-1-AL.

5 References

- Atkinson R., D.L. Baulch, R.A. Cox, R.F. Hampson Jr., J.A. Kerr and J. Troe Evaluated kinetic and photochemical data for atmospheric chemistry: Supplement III, *J. Phys. Chem. Ref. Data* 18, pp 881-1097, 1989.
- Atkinson R. Review article: Gas-phase chemistry of organic compounds: a review. *Atmos. Environment* Vol. 24A, No. 1, pp 1-41, 1990.
- Chang J.S., R.A. Brost, I.S.A. Isaksen, S. Madronich, P. Middleton, W.R. Stockwell and C.J. Walcek A three-dimensional acid deposition model; Physical concepts and formulation. *J. Geoph. Res.* Vol. 92, No. D12, pp. 14,861-14,700, 1987.
- Crutzen P.J. and P.H. Zimmermann The changing photochemistry of the troposphere *Tellus*, Vol 43 A³, pp.136-151, 1991.
- Grennfeldt P., J. Saltbones and J. Schjoldager Oxidant data collection in OECD-Europe 1985-1987 (OXIDATE). *NILU report*, OR 22/87, Lillestrøm, Norway, 1987.
- Guicherit R. Ozone on an urban and regional scale, with special reference to the situation over the Netherlands. *Tropospheric ozone* (ed. Isaksen I.S.A.). NATO ASI Series C, vol.227, pp.49-63, D.Reidel Publishing Company, Dordrecht, 1988.
- Hesstvedt E., Ø Hov and I.S.A. Isaksen Quasi steady-state approximation in air pollution modelling: Comparison of two numerical schemes for oxidant prediction. *Int. Journal of Chem. Kinetics*, Vol X, pp 971-994, 1978.
- Isaksen I.S.A., K.H. Midtbø, J. Sunde and P. Crutzen A simplified method to include molecular scattering and reflection in calculations of photon fluxes and photodissociation rates. *Geophysica Norvegica* Vol. 31, No. 3, 1977.
- Isaksen, I.S.A. Ø. Hov Calculations of trends in the tropospheric concentrations of O₃, OH, CO, CH₄ and NO_x. *Tellus*, Vol 39B, pp.271-283, 1987.
- Jonson J.E. and I.S.A. Isaksen The impact of solar flux variations on the tropospheric ozone chemistry. *Institute report no. 81* Inst. for Geophysics, University of Oslo, 1991.
- Kley D., A. Volz og Mülheims F. Ozone measurements in historic perspective. *Tropospheric ozone* (ed. Isaksen I.S.A.). NATO ASI Series C, vol.227, pp.63-72, D.Reidel Publishing Company, Dordrecht, 1988.
- Lubkert B. and W. Schopp A model to calculate natural VOC emissions from forests in Europe. *International Institute for applied system analysis*. Working paper WP-89-082.
- Prather M. Numerical advection by conservation of second-order moments. *J. Geoph. Res.* Vol. 91, No. D6, pp 6671-6681, May 1986.
- Prather M., M. McElroy, S. Wofsy, G. Russel and D. Rind Chemistry of the global troposphere: fluorocarbons as tracers of air motion. *J. Geoph. Res.* Vol. 92, pp 6579-6613, 1987.
- S. Solberg, I.S.A. Isaksen and R.B. Chatfield Design of a channel model to assess mid-latitude pollution effects. *Proceedings of International Ozone Symposium 1988*. pp 548-551, A. Deepak publ., Virginia, USA, 1989.
- Veldt C. Inventoring natural VOC emissions for the CONAIR project. *TNO-report 88-275*, 1988.
- Watson R.T., M.J. Kurylo, M. Prather and F.M. Ormond Present state of knowledge of the upper atmosphere 1990: An assessment report. *NASA reference publication*, 1242, Sept. 1990.
- Watson J.J., J.A. Probert, S.D. Piccot, J.W. Jones Global inventory of volatile organic compound emissions from anthropogenic sources. *EPA-report EPA-600/8-91-002*, 1991.